Ceramics International **22** (1996) 281–286

0272-8842(95)00102-6
0272-8842/96/$15.00

Tetragonal and Rhombohedral Phase Co-existence in the System: $PbZrO_3$–$PbTiO_3$–$Pb(Fe_{1/5}, Ni_{1/5}, Sb_{3/5})O_3$

A. Boutarfaia & S. E. Bouaoud

Institut de Chimie, Département de Chimie Inorganique, Université de Constantine, Route Ain El Bey, Constantine (25000), Algeria

(Received 24 March 1995; accepted 21 July 1995)

Abstract: Various compositions of $x PbZrO_3$–$y PbTiO_3$–$z Pb(Fe_{1/5}, Ni_{1/5}, Sb_{3/5})O_3$ piezoelectric ceramics, having a Zr/Ti ratio between 45.1/49.9 and 51.1/43.9, were prepared using the usual ceramics technique, in the temperature range 850–1200°C. The electromechanical coupling factor (k_p), piezoelectric constant (d_{ij}) and Young's modulus (Y) are measured as a function of the Zr/Ti ratio. The obtained results are discussed on the basis of the effects of varying the Zr/Ti ratio. The effects of sintering temperature on microstructure are studied by means of a scanning electron microscope (SEM). Grain growth is enhanced by increasing temperature. X-ray diffraction demonstrated the co-existence of both tetragonal and rhombohedral phases. The lattice parameter measurements showed that tetragonal and rhombohedral unit cells of the two phases depend on the sintering temperature.

1 INTRODUCTION

Piezoelectric lead titanate zirconate ceramics, whose composition is near the morphotropic (tetragonal–rhombohedral) phase boundary (MPB), are used in practice because of high values of dielectric constant (ϵ), moduli of piezoelectricity (d_{ij}) and electromechanical coupling factor (k_p).[1–3] Many compounds with the perovskite structure, such as $Pb(Zr,Ti)O_3$, are interesting because of their use in electric devices.[4] Basic physical properties of such materials depend, primarily, on their chemical composition and, in particular, on the Zr/Ti concentration ratio and the presence of impurities.

In the practical applications of PZT, various impurities have been added in order to improve the piezoelectric properties. Some researchers investigated the effect of small amounts of impurities on dielectric and piezoelectric properties of perovskite materials. The grain size has a significant effect on the piezoelectric properties of the sintered ceramics.[5] Also, it is interesting to observe the influence of the calcination and heat treatment conditions on the density, which increases with increasing temperature and time.[6]

Investigations of the $Pb(Zr_x,Ti_{1-x})O_3$ system have shown the existence of an almost temperature-independent morphotropic phase boundary at $x = 0.535$, which separates a rhombohedral phase (R) from a tetragonal one (T).[1,2] By means of X-ray diffraction, the co-existence of the two phases (tetragonal–rhombohedral) over a range of compositions around MPB was demonstrated.[7–15] The aim of this study was to substantially reduce the sintering temperature and to possibly enhance the properties of the materials.

The influence of technological factors on the width of the co-existence region was investigated on the ternary system by X-ray diffraction, because this system is likely to provide a narrow width. It has been found that the MPB is not a vertical straight boundary but a range whose width depends on firing temperature and time.

The present study was done to determine the optimum firing temperature and effects of sintering temperature on the grain size for the ceramics, using results of density and microstructural observation.

The goal of our investigation was to study the morphotropic phase boundary on the basis of X-ray diffraction and variations in electromechanical properties of these ceramics with a view to establish the MPB composition.

2 EXPERIMENTAL

Reagents of Pb_3O_4, ZrO_2, TiO_2, Fe_2O_3, NiO and Sb_2O_3 were mixed to form the composition xPbZrO$_3$–yPbTiO$_3$–zPb(Fe$_{1/5}$, Ni$_{1/5}$, Sb$_{3/5}$)O$_3$ (abbreviated as PZT–PFNSb), where $x+y+z=100\%$, $45.1<x<51.1$, $43.9<y<49.9$ and $z=5\%$ (constant) near the morphotropic phase boundary.

Piezoelectric ceramic samples were prepared by the usual ceramic technique. A mixture of the starting powders was milled and mixed in a vibratory mill, the oxide powders were wet homogenized in distilled water for 10 h and pressed at 1200 kg/cm^2 in preformed pellets of about 15–20 mm high and 13 mm diameter. After mixing, pre-firing of the powders took place at 850°C for 2 h. This was followed by dry ball-milling for 30 h.

The fired powders were pressed into disks of 13 mm diameter and 0.8–1 mm thickness at 14000 kg/cm^2. Finally, the disks were fired in a covered alumina crucible at various sintering temperatures between 850°C and 1200°C for 2 h. Heating rates were 1–5°C/min. The atmosphere was enriched in PbO vapour using $PbZrO_3$ pellets. In general, the weight change of a specimen was less than 2%. Specimens with less than 0.1% weight change were considered to be matured. In addition to the absorption, the linear shrinkage and the apparent density were measured as indications of maturity. Densities were calculated from the mass and dimensions.

After sintering, the silver electrodes were screen printed on to the faces of specimens and fired on at 750°C for 30 min. They were poled in silicone oil at 110°C by applying a static field of 35 kV/cm for 60 min.

Properties such as k_p, S_{11} and d_{31} were measured according to the procedure described in the IRE standards on piezoelectric crystals.[17] The elastic compliance and the electromechanical coupling factor were measured by the resonance–antiresonance method.

The microstructures of the samples were analyzed by means of a scanning electron microscope (SEM), and images were obtained on the fractured surface of the specimens. To establish the difference between tetragonal, rhombohedral and tetragonal–rhombohedral phases, the size distribution of the grains was measured and the results compared with each other.

The crystallographic phases present in the compositions were established by XRD analysis. The samples for analysis were reacted in the alumina crucibles. Heating/cooling rates were 1–6°C/min, and the temperatures were 850, 950, 1050, 1150 and 1180°C. These samples were broken up and ground in a mortar, and the examination was made with a SIMENS D500 diffractometer using CuKα radiation with a nickel filter. The compositions of the PZT phases were identified by an analysis of the peaks [(002)T, (200)R, (200)T] in the 2θ range 43–46. The tetragonal, rhombohedral and tetragonal–rhombohedral phases were characterized and their lattice parameters were calculated. In order to ensure an accurate determination of the lattice parameters, the X-ray peaks were recorded with 0.01°-steps. The data obtained were averaged and smoothed out using a computer. The bulk density of ceramic samples sintered at 1180°C was 7.72×10^3 kg/m^3 and the average grain size was 12–14 μm.

3 RESULTS AND DISCUSSION

Figure 1 shows the effect of sintering temperature on the grain size and the sintered density of samples. It shows that the density increased with temperature. The optimum firing temperature for the maximum density, ρ, of the ceramic is found between 1150 and 1200°C. The maximum density for samples obtained at 1180°C is $\simeq$96.5% of the theoretical value. Theoretical density was assumed to be 8.00×10^3 kg/m^3. Sintering at 1200°C caused the density to decrease. The optimum sintering temperature was taken as the point when the PbO

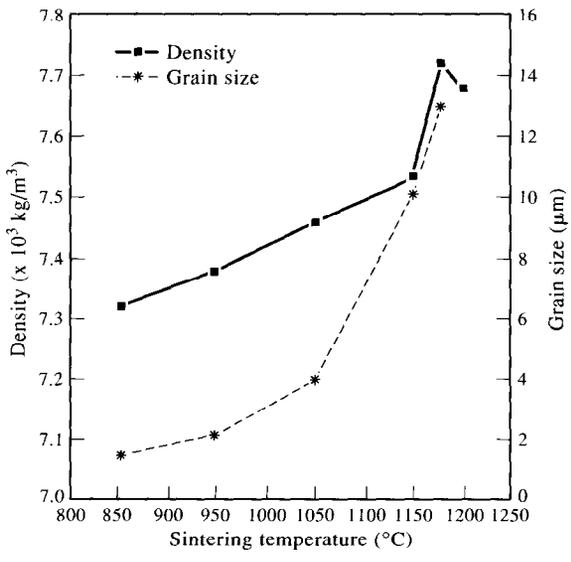

Fig. 1. Effects of sintering temperature on grain size and density (ρ) for PZT–PFNSb ceramics.

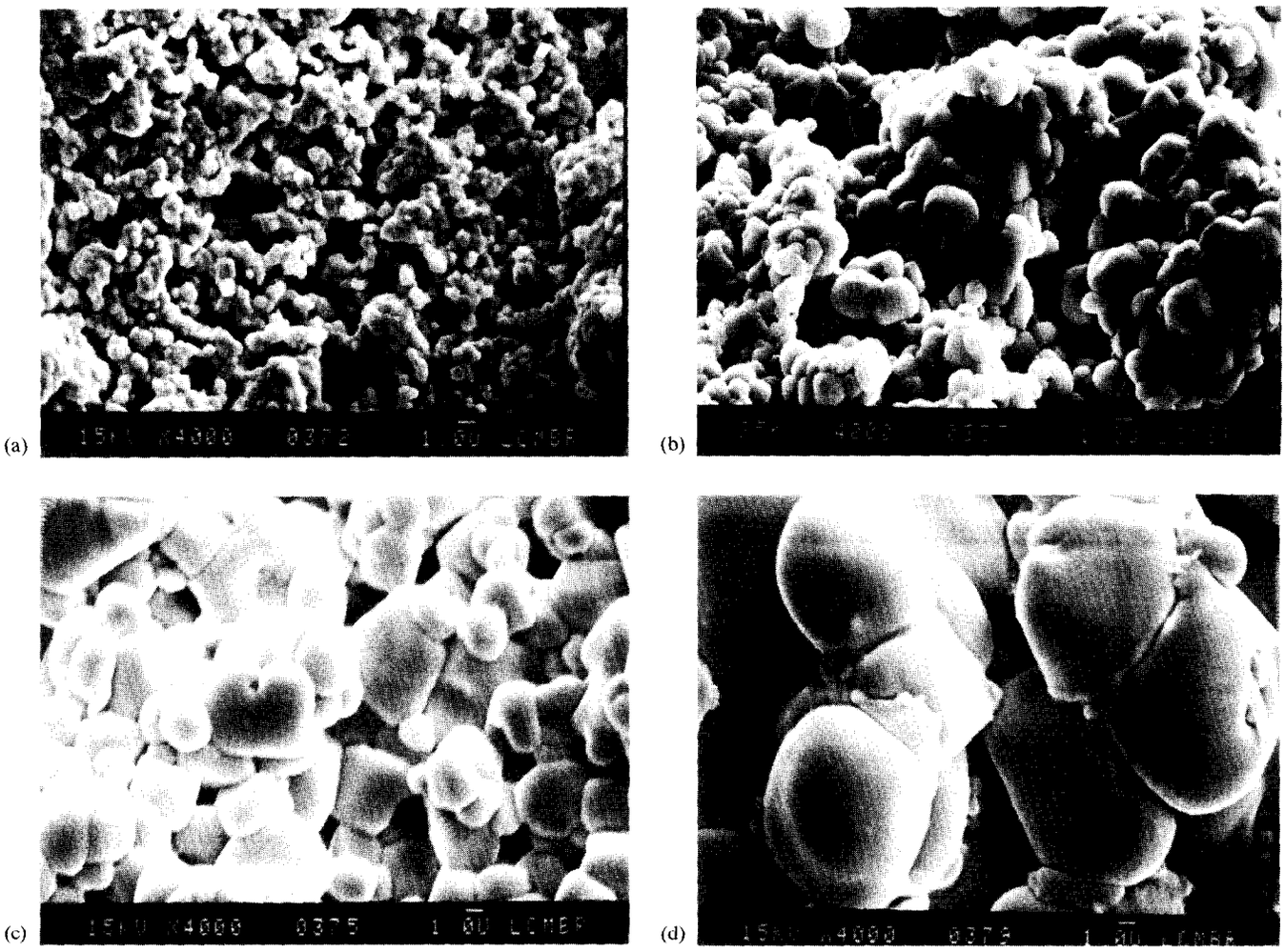

Fig. 2. SEM images of fracture surfaces of PZT–PFNSb ceramics, sintered at (a) 850°C, (b) 950°C, (c) 1050°C and (d) 1180°C.

vapour pressure evaporation–recondensation equilibrium was established. The optimum value of the sintering temperature was affected by the additions of impurities and other processing parameters, such as the rate of heating, time of thermal treatment, and protecting atmosphere.

The grain size increased continuously (exponential form) with sintering temperature for both samples (Fig. 1). The microstructure and grain size were investigated from the SEM images shown in Fig. 2. Small crystallites in the samples sintered at 850°C were noticed, having similar dimensions to those of the initial powder. For the lower sintering temperature (950°C), the average grain diameters have practically the same values (1–2 μm), but for the higher temperatures (1150–1180°C), these values are much more important (10–12 μm or 12–14 μm) than those previously found (5–6 μm).[6]

SEM comparative images show the grain size of sintered ceramic samples at different temperatures. The obtained images show a slight difference in the particle size and also give the different phases, viz. tetragonal, rhombohedral and tetragonal–rhombohedral phases. As well as the morphological modification of grains, different grain sizes could be noticed for these samples. In this way the co-existence region of tetragonal–rhombohedral phases was demonstrated.

The compositional fluctuations can lead to the formation of very small regions rich in tetragonal (lead titanate) grains of ceramics. We also observed the existence of islands of the rhombohedral phase. This corresponds to the morphotropic phase boundary. At the same time, we observed tetragonal islands on rhombohedral (lead zirconate) grains of the same sample. Let us call these islands 'regions of different symmetry'. All this happened as a function of microscopic concentration and temperature gradients.[12–14]

Variations in the values of the electromechanical properties as a function of the Zr/Ti ratio are representated in Fig. 3. It can be noticed from the curves that k_p and d_{31} reach maximum values, and $1/S_{11}$ (reciprocal elastic compliance) shows a minimum at a Zr/Ti ratio of 47.1/47.9 in the solid solution. Thus from the trend of the variation of

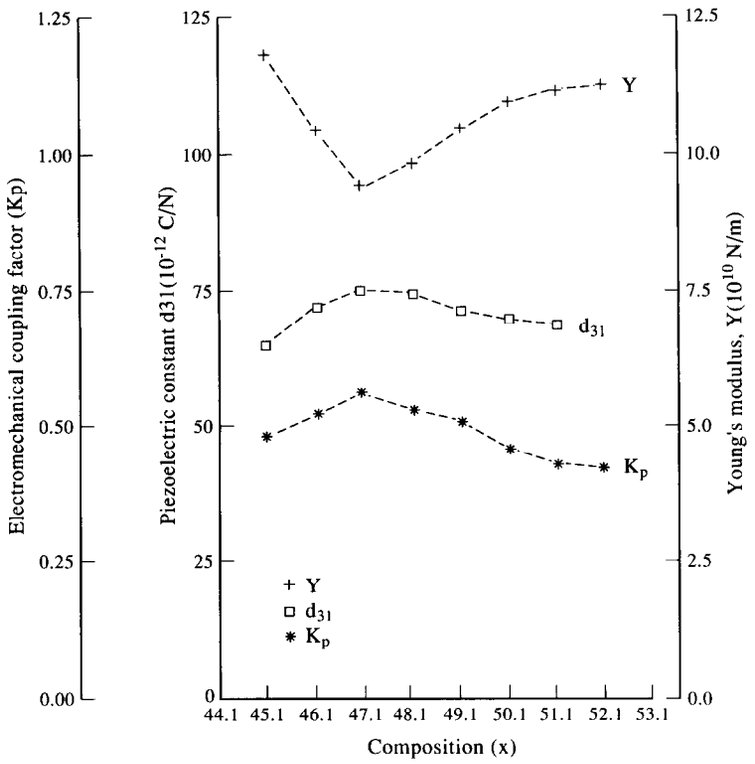

Fig. 3. Variation of k_p, d_{31} and Y with composition (x) for PZT–PFNSb solid solutions.

electromechanical properties and their optimum values, it is obvious that the MPB lies at approximately 47.1/47.9:Zr/Ti ratio in PZT ceramics. From the behaviour of the elastic compliance it is evident that $1/S_{11}$ cannot contribute fully, assuming that during poling a higher domain alignment degree is achieved in the co-existence region of tetragonal and rhombohedral phases.

Reciprocal elastic compliance (Young's modulus) of the system is shown in Fig. 3 with an increasing Zr/Ti ratio. It can be seen that the curve is characterized by a minimum near the phase transition. This could be explained by the gradual decrease of tetragonality and a pronounced drop of the curve near the phase transition (47.1/47.9:Zr/Ti).

The X-ray diffraction spectra of samples, sintered at temperatures ranging from 850°C to 1180°C, showed in all cases the co-existence of both tetragonal and rhombohedral phases, which are characterized by reflections splitting in triplets of type (002)T, (200)R and (200)T (Fig. 4).

The fact that the diffraction lines were split into triplets for the samples indicated that the co-existence region of both ferroelectric phases at MPB was not altered by the oxide additions.

The lattice parameters a_T and c_T of the tetragonal structure and a_R of the rhombohedral structure were calculated from the triplets (200). By increasing the sintering temperature, the position of the two tetragonal peaks tends to move closer to the rhombohedral one which has a mean position.

The results obtained for the 48.1 $PbZrO_3$–46.9 $PbTiO_3$–5 $Pb(Fe_{1/5}, Ni_{1/5}, Sb_{3/5})O_3$ solid solutions showed that the lattice parameters of the tetragonal phase changed with sintering temperature (Fig. 5). The value of the a_T parameter increased from 4.0362 Å to 4.0416 Å, and the c_T parameter value decreased from 4.1198 Å to 4.1158 Å, when the sintering temperature increased from 850°C to 1180°C. The resulting values of the lattice parameters of the tetragonal phase showed that the c_T/a_T axial ratio decreases as a_T increases and c_T decreases. The lattice parameters for the rhombohedral phase were only slightly modified compared to the ideal structure. The values of the lattice parameters were found to be practically the same as those previously studied.[15] The variation of the lattice parameters as a function of sintering temperature could be explained by the enhancement of cation diffusion and therefore by the homogenization of solid solutions. The impurities did not affect the crystalline structure.

Some researchers have reported the possible co-existence of an extended region of the morphotropic phase boundary composition, where tetragonal and rhombohedral phases are both stable.[9] The tetragonal form is stable over the composition range from $x = 0$ to $x = x_T$, and the rhombohedral form from $x = x_R$ to $x = 1$, where $x_R < x_T$. The width, $\Delta x = x_T - x_R$, of the 'co-existence region' is close to that obtained in different studies.[12–14]

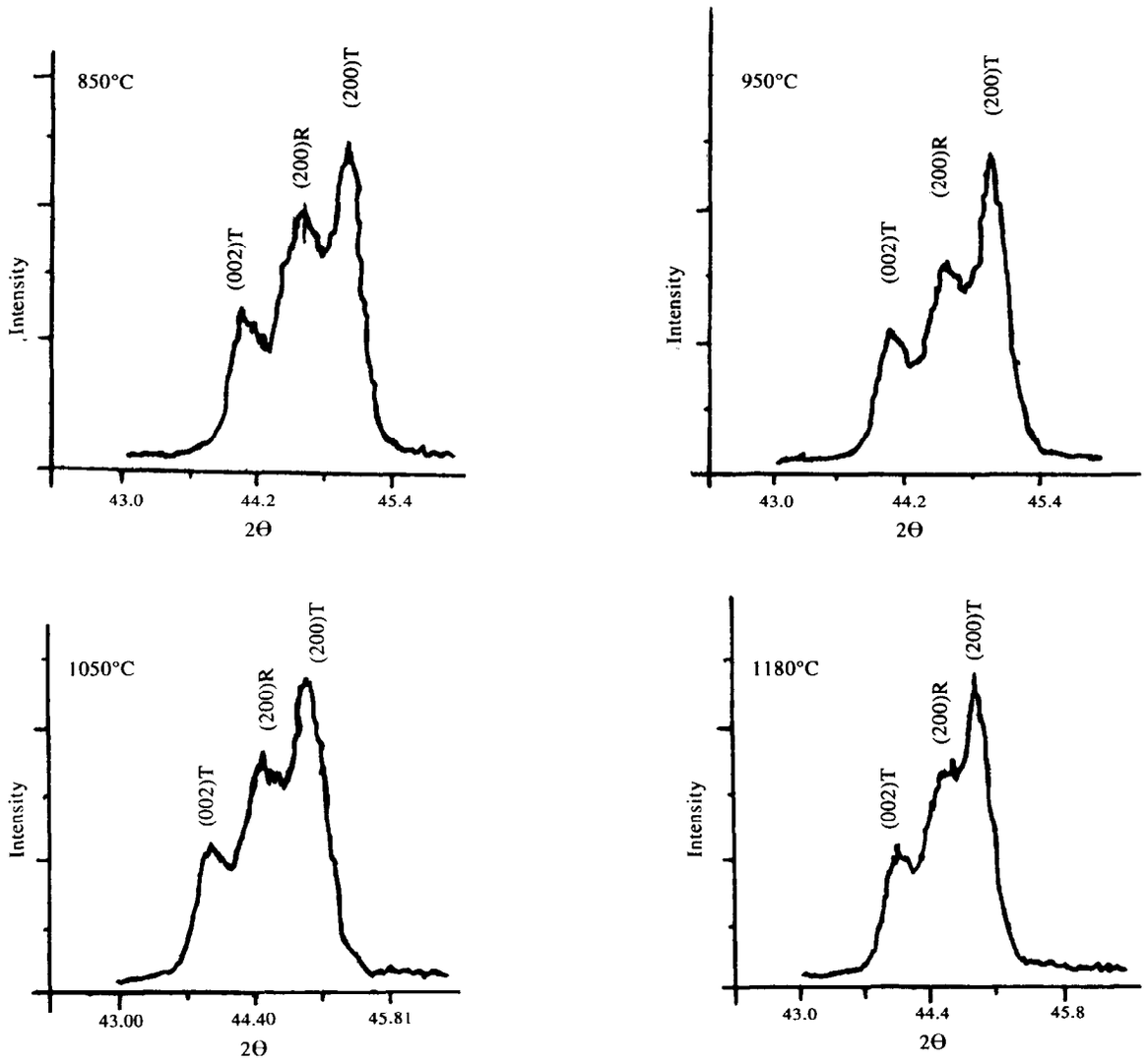

Fig. 4. Typical X-ray diffraction patterns obtained for PZT–PFNSb ceramics sintered at 850, 950, 1050 and 1180°C, showing triplets (002)T, (200)R and (200)T.

In Fig. 6, we can see that the width of the co-existence region can be reduced with sintering temperature, and in Fig. 5 the variation in the lattice parameters of the identified phase composition shows that the values of the c_T/a_T ratio have decreased. This can be explained by microscopic compositional fluctuations occurring in these perovskite materials, which cannot provide a real homogeneity in the solid solutions, and also by the different stresses induced in the ceramic grains, which determined the co-existence of tetragonal–rhombohedral phases. The increase of sintering temperature and firing time enhanced the diffusion effects within these regions and led to a relative homogenization of the local composition in the material. Thus the improvement in electromechanical properties with the change in the Zr/Ti ratio of PZT compositions (shown in Fig. 3) can be attributed to the decrease in the values of the c_T/a_T ratio of the tetragonal phase.

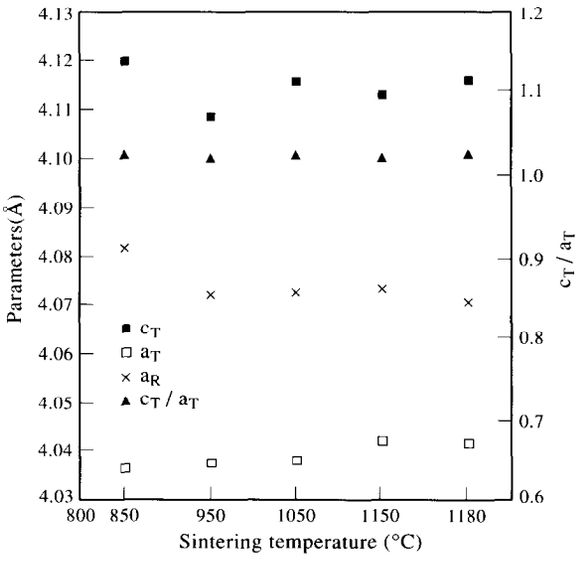

Fig. 5. Lattice parameters variations for both co-existence phases as a function of sintering temperature.

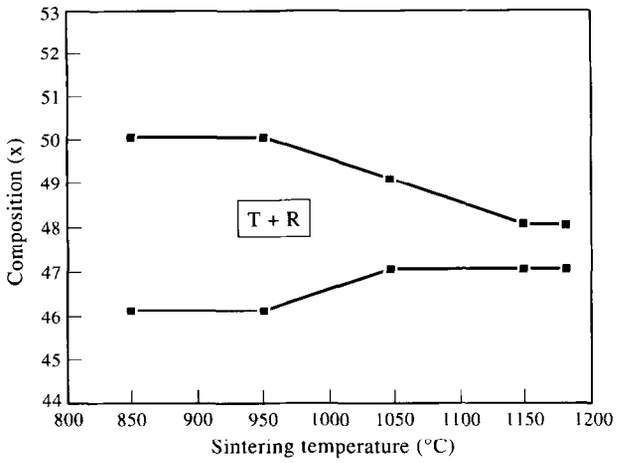

Fig. 6. Variation of the width of the co-existence region as a function of sintering temperature.

4 CONCLUSIONS

The study of the morphotropic phase boundary has established that the phase transition from tetragonal to rhombohedral symmetry in $x\text{PbZrO}_3 - y\text{PbTiO}_3$–$z\text{Pb}(\text{Fe}_{1/5}, \text{Ni}_{1/5}, \text{Sb}_{3/5})\text{O}_3$ takes place at $x = 47.1$ and the width of the phase boundary has been found to be in the range of $47.1 < x < 48.1$ at 1180°C. The co-existence region was investigated by X-ray diffraction. It was found that the MPB is not a narrow and vertically straight boundary but a region whose width depends on the firing temperature.

The lattice parameters a_T and c_T of the tetragonal structure and a_R of the rhombohedral structure were found to vary with sintering temperature.

The effect of sintering temperature on the density and grain size of PZT–PFNSb ceramics has been investigated. It was demonstrated that the grain size increased continuously with sintering temperature. Experimental results have shown that PZT–PFNSb ceramics have uniform microstructures and high density, 7.72×10^3 kg/m^3, at a sintering temperature of 1180°C.

In this investigation the tetragonal–rhombohedral phases co-existence in the system showed that the coupling factor (k_p) and piezoelectric constant d_{31} are higher when they get close to the tetragonal–rhombohedral phase boundary.

REFERENCES

1. SAWAGUCHI, E., *J. Phys. Soc. Jpn*, **8** (1953) 615.
2. JAFFE, B., ROTH R. S. & MARZULLO, S., *J. Res. Natl Bur. Stand.*, **55** (1955) 239.
3. PINCZUK, A., *Solid State Commun.*, **12** (1973) 1035.
4. KAKEGAWA, K. & MOHRI, J., *J. Am. Ceram. Soc.*, **68** (1985) C-204.
5. OKAZAKI, K. & NAGATA, K., *J. Am. Ceram. Soc.*, **56** (1973) 82.
6. BUCKNER, D. A. & WILCOX, P. D., *Am. Ceram. Soc. Bull.*, **52** (1972) 218.
7. CARL, K. & HARDTL, K. H., *Phys. Status Solidi (a)*, **8** (1971) 87.
8. ISUPOV, V. A., *Solid State Commun.*, **17** (1975) 1331.
9. KAKEGAWA, K., MOHRI, J., TAKAHASHI, K., YAMAMURA, H. & SHIRASHAKI, S., *Solid State Commun.*, **24** (1977) 769.
10. ARI-GUR, P. & BENGUIGUI, L., *Solid State Commun.*, **15** (1974) 1077.
11. ARI-GUR, P. & BENGUIGUI, L., *J. Phys. D.*, **8** (1975) 1856.
12. BENGUIGUI, L., *Solid State Commun.*, **11** (1972) 825.
13. ISUPOV, V. A., *Soviet Physics Solid State*, **10** (1968) 989.
14. KINGON, A. I., TERBLANCH, P. J. & CLARK, J. B., *Ceram. Int.*, **8** (1982) 108.
15. MABUD, S. A., *J. Appl. Cryst.*, **13** (1980) 211.
16. WITTMER, D. E. & BUCHMAN R. C., *J. Am. Ceram. Soc.*, **64** (1981) 485.
17. IRE standard on Piezoelectric Crystals, *Proc. IRE (Inst. Radio Engrs)*, **49** (1961) 1161.